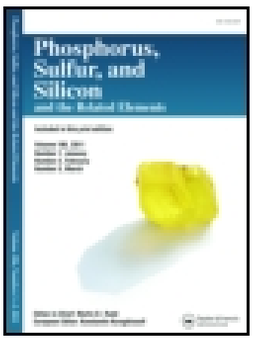

Taylor & Francis
Taylor & Francis Group

Phosphorus, Sulfur, and Silicon and the Related Elements

ISSN: 1042-6507 (Print) 1563-5325 (Online) Journal homepage: https://www.tandfonline.com/loi/gpss20

Novel dibenzosuberene substituted aroyl selenoureas: Synthesis, crystal structure, DFT, molecular docking and biological studies

Moideen Musthafa, Ramaiah Konakanchi, Rakesh Ganguly & Anandaram Sreekanth

To cite this article: Moideen Musthafa, Ramaiah Konakanchi, Rakesh Ganguly & Anandaram Sreekanth (2019): Novel dibenzosuberene substituted aroyl selenoureas: Synthesis, crystal structure, DFT, molecular docking and biological studies, Phosphorus, Sulfur, and Silicon and the Related Elements, DOI: 10.1080/10426507.2019.1699924

To link to this article: https://doi.org/10.1080/10426507.2019.1699924

PHOSPHORUS, SULFUR, AND SILICON AND THE RELATED ELEMENTS
https://doi.org/10.1080/10426507.2019.1699924

Novel dibenzosuberene substituted aroyl selenoureas: Synthesis, crystal structure, DFT, molecular docking and biological studies

Moideen Musthafa[a], Ramaiah Konakanchi[b], Rakesh Ganguly[c], and Anandaram Sreekanth[a]

[a]Department of Chemistry, National Institute of Technology, Tiruchirappalli, India; [b]Chemistry Division, H&S Department, Vignan Institute of Technology and Science, Deshmuki, Hyderabad, India; [c]Division of Chemistry & Biological Chemistry, Nanyang Technological University, Singapore, Singapore

ABSTRACT

A series of aroyl selenourea dibenzosuberene **(1–3)** derivatives were synthesized and characterized by different analytical methods and single crystal X-ray crystallography. Quantum chemical computations were made using DFT to determine the structural and molecular properties of the compounds. The *in vitro* antibacterial action of the compounds was evaluated against chosen gram-negative (*Pseudomonas aeruginosa*, *Klebsiella pneumoniae*, and *Escherichia coli*), and gram-positive (*Bacillus subtilis*, *Staphylococcus aureus*, and *Staphylococcus epidermidis*) bacteria for their antifungal activity against *Curvularia lunata, Penicillium notatum*, and *Aspergillus niger*. Using molecular docking studies, the binding modes were understood along with the mechanism in opposing the target protein MurB.

ARTICLE HISTORY
Received 10 September 2019
Accepted 28 November 2019

KEYWORDS
Antibacterial; antifungal; molecular docking; DFT; single-crystal XRD

GRAPHICAL ABSTRACT

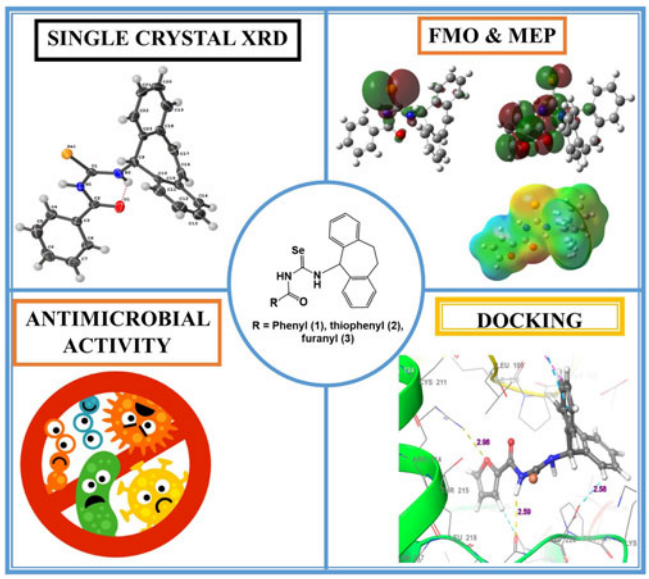

1. Introduction

Selenium is known as a biological trace element for the development and well-being of animals and humans.[1] Health benefits have attracted the most attention to selenium, as it is a cancer prevention agent.[2,3] Over the past four decades, epidemiological studies have shown low mortality rates in areas with high levels of selenium. Selenium is known primarily for its antioxidant function and its healing, chemopreventive, anti-inflammatory, and anti-virus properties.[4] Selenium's antinuclear properties have been proven in most animals and *in vitro* studies, mostly at nutritional levels. Additionally, there is a possibility of not only selenium front prevention but also cancer treatment.[5,6] Over the past decade, novel agents have emerged as anticancer agents of them, selenium, which has molecules, has shown a greater interest in cancer prevention and protection.[7]

CONTACT Anandaram Sreekanth sreekanth@nitt.edu Department of Chemistry, National Institute of Technology, Tiruchirappalli, 620015, India; Rakesh Ganguly rganguly@ntu.edu.sg Division of Chemistry & Biological Chemistry, Nanyang Technological University, Singapore, 639798, Singapore.
Color versions of one or more of the figures in the article can be found online at www.tandfonline.com/gpss.
Supplemental data for this article is available online at https://doi.org/10.1080/10426507.2019.1699924.

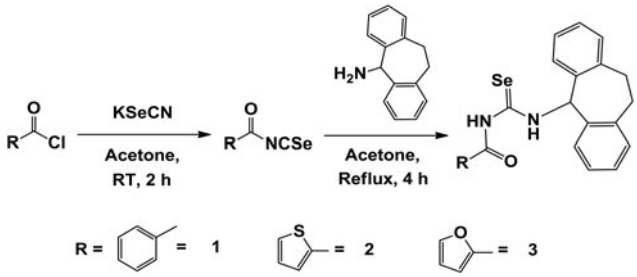

Scheme 1. Synthesis of aroyl selenourea compounds **(1–3).**

Organic derivatives that include selenium have other medical applications, and are biologically active substances with anti-viral, anti-bacterial, antihypertensive, and fungicidal properties.[8] A variety of organoselenium compounds (such as heterocycles, selenocarbamates, and selenoureas), among them, selenourea derivatives are significant candidates.[9–12]

Recently, selenoureas have emerged as free radical scavengers, enzyme inhibitors, anticancer agents with other biological aspects.[13–16] Thus selenoureas can be utilized to develop new chemotherapeutic agents.[17–20] Dibenzosuberene (5 *H*-dibenzo[*a*,*d*]cycloheptene) are biologically active molecules. Generally, bulky compounds move through a sterile shelter to mobilize a movement and increase the penetration of lung by lipophilicity.The steric characteristics of dibenzosuberene resembles 5 H-dibenzo[b,-f]azepine-5-carboxamide (Carbamazepine), and is used as an anticonvulsant or antiepileptic drug.[21–24] The compounds **(1–3)** were represented by utilizing different spectroscopic systems. Computational investigations were performed using DFT studies to get data of the fundamental properties of the compounds, from which we undertook FMO and MEP studies. The HOMO and LUMO energies were also evaluated to demonstrate the chemical stability of the molecules. *In vitro* antibacterial and antifungal activity studies of the new compounds were investigated.

2. Results and discussion

2.1. Synthesis

The 5 H-dibenzo[a,d][7]annulen-5-amine was prepared according to standard procedure (Figure S1, supplementary material).[25] The new *N*-dibenzosuberene substituted aroyl selenoureas **(1–3)** were prepared by adopting the reported method (Scheme 1).[26]

2.2. Characterizations

The electronic spectra of the compounds **(1–3)** showed absorption bands around 270–283 nm, and 314–324 nm corresponding to $\pi \rightarrow \pi^*$ and $n \rightarrow \pi^*$, transitions (Table S1, supplemental materials). The UV–visible spectra of the compounds **(1–3)** are shown in Figure S2 (supplementary material). The Fourier-transform-infrared spectra of the compounds **(1–3)** (Table S2, supplementary material) showed peaks in the range of 3370–3398 cm^{-1} corresponding to amide N – H. Aroyl selenourea N – H appeared at 3294–3311 cm^{-1}.C = O stretch frequencies were observed in 1657–1670 cm^{-1}. The characteristic absorption of C = Se vibrations appeared in the range of 1156–1167 cm^{-1}, which agrees with previously reported compounds.[27] The FTIR spectra of the compounds **(1–3)** are shown in Figure S3 (supplementary material).

^{1}H NMR spectra of the compounds revealed that the N – H proton between carbonyl and selenocarbonyl group appeared as singlets around 9.04–9.15 ppm and peaks in the range of 11.64–11.89 ppm were assigned to N – H proton present between selenocarbonyl and suberenyl sp^3 carbon. Peaks in the region of 6.93–6.29 ppm were assigned to suberenyl N – CH proton. The aromatic protons appeared as multiplets in the region 6.15–7.78 ppm. Signals at 178.5–179.0 ppm (C = Se) and at 156.9-166.4 ppm (C = O) respectively appeared in the ^{13}C NMR spectrum. The aromatic carbons of aroyl selenourea were observed in the range of 112.0–146.1 ppm. ^{77}Se NMR spectra of the compounds revealed C = Se peaks in the region of 417.20–404.02.The spectra are shown in Figure S4 (^{1}H NMR, supplementary material), Figure S5 (^{13}C NMR, supplementary material), and Figure S6 (^{77}Se NMR), Mass spectra of the compounds **(1–3)** are shown in Figure S7 (supplementary material).

2.3. Single-crystal XRD analysis

The molecular structures of compounds **1** and **2** were further confirmed by single-crystal XRD studies. The crystal refinement parameters of **(1-2)** are given in Table S3 (supplementary material). The structures of **(1-2)** with atomic labeling and crystal packing are displayed in Figures 1–3. Selected interatomic bond lengths and bond angles are presented in Tables 1 and 2. The compounds **1** and **2** crystallises into monoclinic and triclinic lattice, respectively, with space groups P121/n1 and P-1. The crystal structures of **1** and **2** revealed a possible intramolecular hydrogen-bonding interaction between the carbonyl group and N (2)–H. Furthermore, the selenourea C = Se bond lengths were comparable to earlier reported selenourea compounds indicating less distortions in the molecular structure.[28]

2.4. DFT studies

2.4.1. MEP analysis

Molecular electrostatic potential (MEP) maps describe the charge density of molecules three-dimensionally and predict nucleophilic and electrophilic centers in them .[29–31] The MEP V(r) at a point r is represented as [32,33]

$$V(r) = \Sigma^{N}{}_{A}\left[(Z_A/|r - R_A|) - \int \rho\ (r')\ d3r'/|r - r'|\right.$$

where N is the total number of nuclei in the molecules. The molecular electrostatic potential of the compounds **(1–3)** is shown in Figure S8 (supplementary material). The graphic illustration with a rainbow color scheme of Molecular electrostatic potential (MEP) is within the range

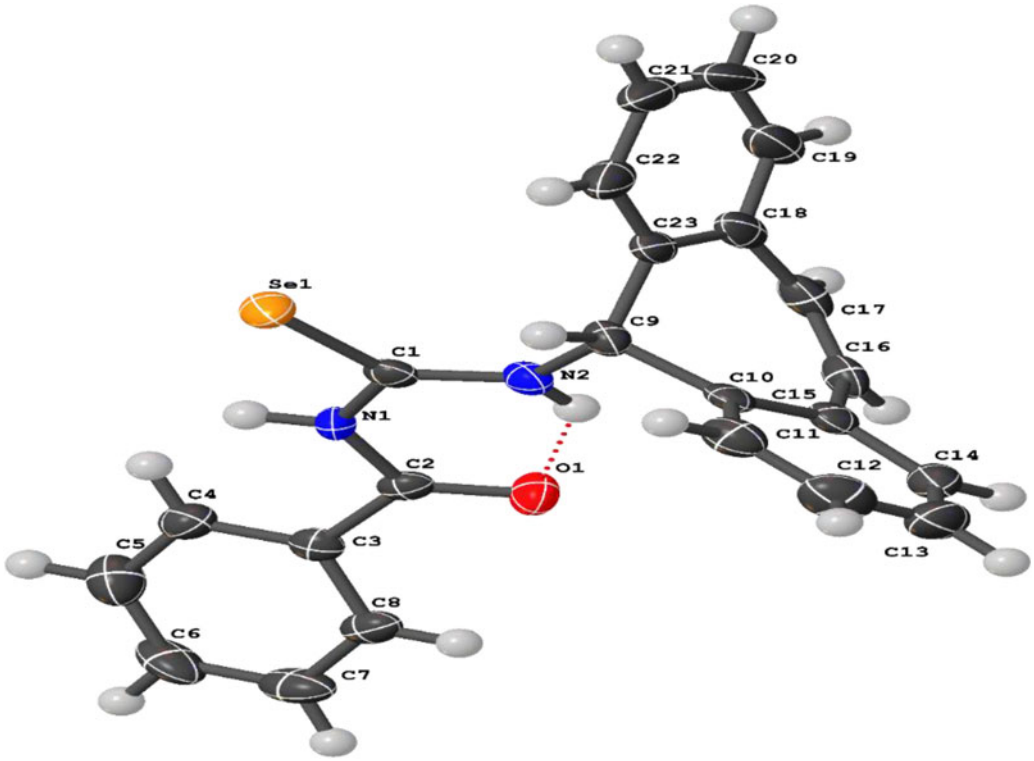

Figure 1. Thermal ellipsoid plot with atomic labeling of 50% probability of **1**.

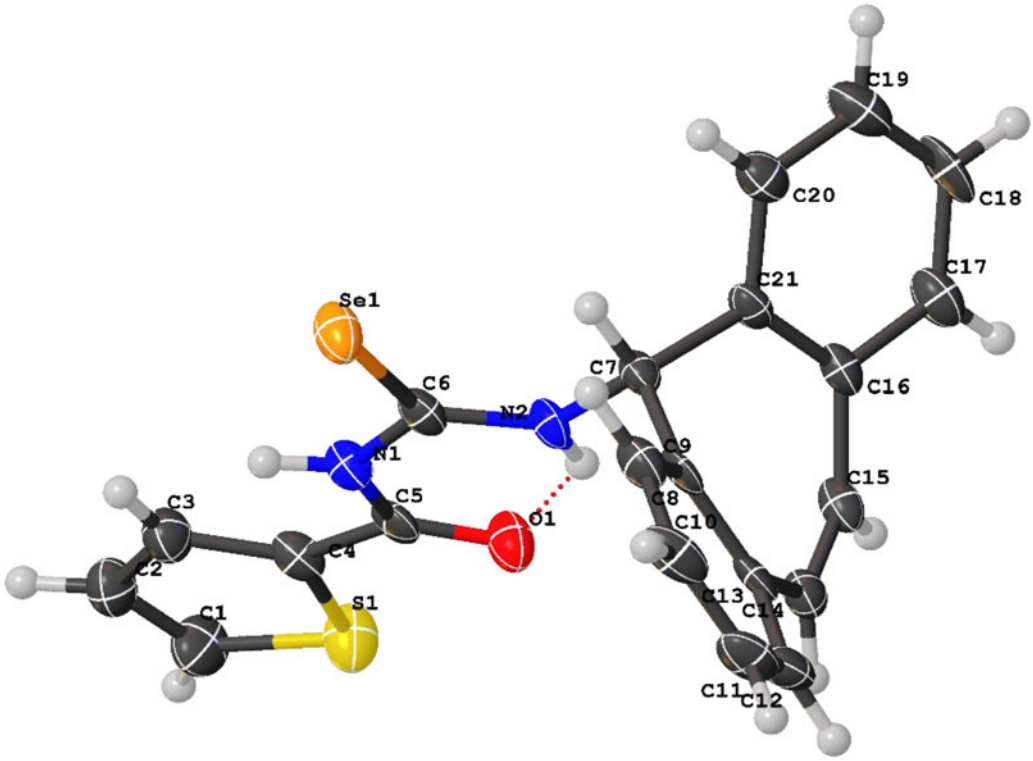

Figure 2. Thermal ellipsoid plot with atomic labeling of 50% probability of **2**.

of -6.138 e^{-2} to $+6.138$ e^{-2}, -6.315 e^{-2} to $+6.315$ e^{-2}, -6.018 e^{-2} to $+6.108$ e^{-2} for **(1–3)**, respectively. The negative potential shows high-electron density is indicated in red in the figure. The low-electron density (positive potential) is indicated in blue. Aroyl selenoureas have high-electron density and are progressively susceptible to electrophilic attack.

2.4.2. Frontier molecular orbital analysis

Frontier molecular orbitals (HOMO and LUMO) and their energies are important parameters for spectroscopists in the field of quantum chemistry. LUMO energy represents the ability to accept an electron, HOMO energy is related to the ability to donate an electron. The energy difference between HOMO and LUMO characterizes their molecular

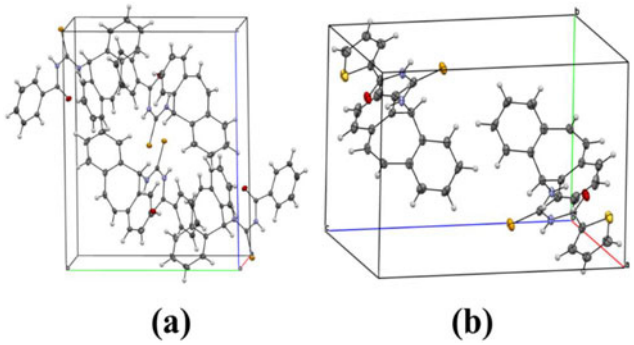

Figure 3. Crystal packing of compounds (a) **1** and (b) **2**.

Table 1. Bond lengths (Å) and bond angles (°) selected for **1**.

Bond lengths (Å)			
Se1-C1	1.829(2)	C2-O1	1.226(3)
C1-N1	1.379(3)	C2-N1	1.386(3)
C1-N2	1.317(3)	C9-N2	1.474(3)
Bond angles (°)			
O1-C2-N1	122.2(2)	O1-C2-C3	120.8(2)
N1-C2-C3	117.02(19)	N2-C1-N1	115.8(2)
N2-C1-Se1	126.10(17)	N1-C1-Se1	118.08(16)
N2-C9-C10	112.21(18)	N2-C9-C23	107.19(18)
C1-N2-C9	125.10(19)	C1-N1-C8	127.25(19)

chemical stability. Furthermore, the LUMO energy is directly related to electron affinity.[34,35] This is used to estimate frontier electron density predict the most reactive position in π-electron systems. It is also used to explain several types of reactions in conjugated systems.[36] Conjugated molecules are characterized by a small separation between HOMO and LUMO, which is the result of a significant degree of intermolecular charge transfer from the end-capping electron-donor groups to the efficient electron-accepter groups through an π-conjugated path.[37] To understand various aspects of pharmacological formulations including drug design and the possible ecotoxicological characteristics of drug molecules, several new chemical reactivity descriptors have been proposed. Conceptual DFT-based descriptors have helped in many ways to understand the structure of molecules and their reactivity by calculating the chemical potential, global hardness and electrophilicity. Using, HOMO and LUMO orbital energies, the electron affinity (A), ionization energy (I), chemical potential (μ), Global hardness (η), and global electrophilicity power (μ) of a compound can be calculated as [38]

$$A = -E_{\mathrm{LUMO}};\ I = -E_{\mathrm{HOMO}};\ \mu = (E_{\mathrm{HOMO}} + E_{\mathrm{LUMO}})/2;\ \eta = (-E_{\mathrm{HOMO}} + E_{\mathrm{LUMO}})/2 \text{ and } \omega = \mu^2/2\eta.$$

HOMO and LUMO energy values are calculated at B3LYP/6-311++G(d,p) basic set. Energy values of the compounds **(1–3)** are, E_{HOMO} = –5.12, –5.31, and –5.29 eV and E_{LUMO} = –1.59, –1.98, and –1.76 eV, respectively. Energy gaps of HOMO and LUMO in the compounds **(1–3)** are found to be 3.53, 3.33, and 3.53 eV, respectively. The results are represented in Table S4 (supplementary material). According to Parr *et al.*[39] As mentioned, the molecule with small energy gap has more polarization property, low kinetic stability and is in general called a soft molecule. These molecules can be explained as the resistance toward the deformation of electron cloud and polarization of chemical systems during the chemical process. Chemical softness is a useful concept the behavior of chemical systems and is related to their stability and low reactivity. Chemical hardness is a useful concept to predict the behavior of chemical systems and is related to the stability of a chemical system. Global hardness η and chemical potential μ of the compounds are given by using the relation $\eta = (-E_{\mathrm{HOMO}} + E_{\mathrm{LUMO}})/2 = 1.76$, 1.66, and 1.76 eV, $\mu = (E_{\mathrm{HOMO}} + E_{\mathrm{LUMO}})/2 = -3.36$, −3.64, and 3.52 eV and the Electrophilicity index (ω) = $\mu^2/2\eta$ can be interpreted as a measure of energy reduction due to maximal electron flow between the donor and acceptor.[40] Soft molecules have small hardness, while the hard ones have large chemical splitting compounds **(1–3)** Electrophilicity index values are found to be 6.39, 7.98, and 7.04 eV, respectively. The calculated values describe the catalytic and biological activity of the title compound. The atomic orbital components of the frontier molecular orbital are shown in Figure 4.

Table 2. Bond lengths (Å) and bond angles (°) selected for 2.

Bond lengths (Å)			
C6-Se1	1.842(5)	C5-O1	1.231(7)
C5-N1	1.378(7)	C6-N2	1.332(7)
C7-N2	1.474(6)	C6-N1	1.390(7)
C1-S1	1.695(6)	C4-S1	1.714(6)
Bond angles (°)			
C2-C1-S1	112.1(4)	N1-C5-C4	116.1(5)
C3-C4-S1	112.0(4)	N2-C6-N1	117.2(5)
C5-C4-S1	117.2(4)	N2-C7-C8	111.6(4)
O1-C5-N1	123.1(5)	N2-C7-C21	110.8(4)
O1-C5-C4	120.7(5)	C5-N1-C6	126.2(4)
C6-N2-C7	123.1(4)	C1-S1-C4	91.6(3)

2.5. Molecular docking studies

MurB is a flavoprotein, also known as UDP-*N*-acetylenolpyruvoylglucosamine reductase. It catalyzes the decrease of an enolpyruvyl uridine diphosphate-*N*-acetyl glucosamine, which is the second step in the biosynthesis of a bacterial cell's peptidoglycan layer. The reduced product, UDP-*N*-acetyl muraic acid, acts as a locus for peptide portion attachment to the cell wall. These cross-links are responsible for cell rigidity. So MurB is an important enzyme in bacterial cell wall synthesis. We have chosen *E. coli*: MurB (PDB ID: 1MBB) as the target protein, which was recovered (httpww.rcsb.org/pdb) from the Protein Data Bank.[41–43]

Among all compounds, compound **1** exhibited good inhibition activity against the protein 1MBB is indicated by its lower binding energy value −5.31 kcal/mol. The docking results are shown in Table 3. The compound **3** forms three hydrogen bonds and the residues involved in the interaction with compounds are PROA111, PROA219, ARG219, ASPA220, respectively as seen in the figure. Compound **3** also displayed excellent activity against 1MBB protein with binding energy values − 5.63 kcal/mol. The docking poses of

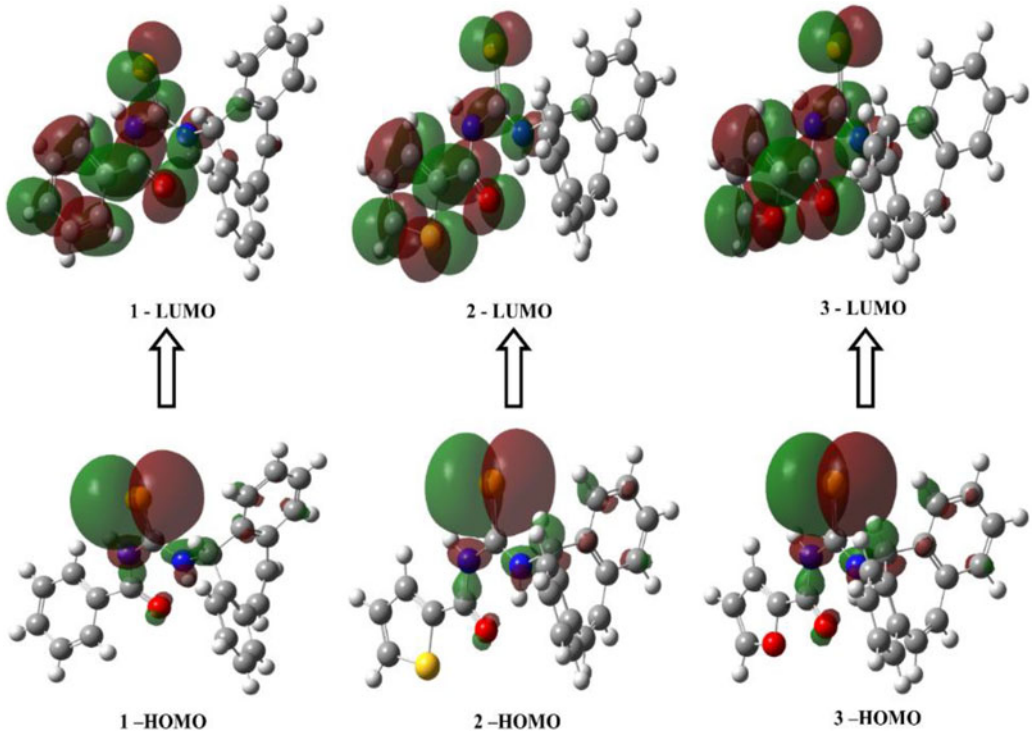

Figure 4. LUMO and HOMO energy level of compounds **(1–3)**.

Table 3. MurB (PDB ID: 1MBB) docking parameters of compounds **(1–3)**.

Compound	No. of rotational bonds	best binding energy (kcal/mol)	Inhibition constant (Ki) μM	Amino acid residues involved in an interaction with compounds
1	3	−5.31	74.35	Pi –Anion : GLU A323 (4.60 Å) Pi-Alkyl : LYS A232 (4.61 Å) Amide – Pi stacked : ASN (2.61 Å) A233 (2.27 Å).
2	3	−4.18	86.62	Pi-Alkyl : PRO A221 (3.85Å), PRO A111 (4.63 Å) Pi –Anion : GLU A48 (5.57Å),ASP A220 (3.27 Å).
3	3	−5.63	128.14	Pi-Alkyl : LYS A222, PRO A221 (4.27 Å) Hydrogen bond : PRO A111 (5.13 Å), PRO A219 (2.59 Å), ARG 219, ASP A220 (3.23 Å). Pi-sigma : LEU A218.

the compounds **(1–3)** with the protein 1MBB are shown in Figures S9–S11 (supplementary material).

2.6. Antimicrobial activity

Compounds **(1–3)** were evaluated for their *in vitro* antimicrobial action against both gram-negative (G^-) and gram-positive (G^+) bacteria strains and different fungal strains[44–47] using Streptomycin and Nystatin as reference controls. The MIC is illustrated in Tables S5 and S6 (supplemental materials). The minimum inhibitory levels are indicated. The information shows that *in vitro* antimicrobial activity was considerable against almost all antibacterial and antimicrobial strains.

Among tested compounds **(1–3)**, compound **3** has a wide range of activity with MIC values of 10.5 µg/mL (*S. aureus*), 11.9 µg/mL (*B. subtilis*), 9.5 µg/mL (*S. epidermidis*), 3.6 µg/mL (*E. coli*), 10.8 (*K. pneumoniae*), and 21.8 (*P. aeruginosa*), respectively, compared to Streptomycin. Compound **1** against *K. pneumoniae*, and compound **2** against *B. subtilis* exhibited moderate activity with MIC values of 18.6 µg/mL and 25.6 µg/mL, correspondingly. Compound **3** showed good activity against *A. niger* with MIC values of 19.4 µg/mL and moderate activity against *P. notatum* and *C. lunata* with MIC values of 11.4 and 24.8 µg/mL, respectively. Compounds **1** and **2** showed medium to low antifungal activity with MIC values of 25.3–63.2 μg/mL against the test strains.

3. Materials and methods

All reagents were purchased from Alfa-Aesar and Sigma-Aldrich. All the solvents were dried and purified according to standard procedures. Elemental analyses (C, H, N, and S) were performed on a Vario EL III Elemental analyzer instrument. UV–visible spectra were recorded in DMF solution using analytic Jena SPECORD S600 spectrophotometer. FT-IR spectra in a range $4000-400\,cm^{-1}$were recorded on a Perkin Elmer FT-IR/FIR Frontier spectrometer. NMR spectra were recorded in $CDCl_3$ or DMSO-d_6 using TMS as an

internal standard on a Bruker 500 MHz spectrometer. Melting points were determined in open capillary tubes on a Lab India melting point apparatus.

4. Experimental section

4.1. Synthesis of N-dibenzosuberene substituted compounds (1–3)

Compounds **(1–3)** were prepared by the following method. A solution of benzoyl chloride (0.6 mL, 5 mmol) or thiophene-2-carbonyl chloride (0.6 mL, 5 mmol) or furan -2-carbonyl chloride (0.5 mL, 5 mmol) in dry acetone (25 mL) was added dropwise to potassium selenocyanate (0.4859 g, 5 mmol) in dry acetone (25 mL). The reaction mixture was stirred for one hour at room temperature. After cooling, dibenzosuberenyl amine (1 g, 5 mmol) dissolved in acetone (30 mL) was added to it dropwise, and the resulting mixture was refluxed for 2 h at 65 °C. The reaction mixture was mixed with into hydrochloric acid (0.1 N, 200 mL) and the resulting pale yellow/brown substance was filtered off. Recrystallisation purified the solid product from a chloroform/ethanol mixture (1/2).

4.1.1. N-((5H-dibenzo[a,d][7]annulen-5-yl)carbamoselenoyl)benzamide (1)

Yield: 1.18 g, 78%. Yellow solid. m.p.: 164 °C. Anal. Calc. for $C_{23}H_{18}N_2OSe$ (%): C, 74.57; H, 4.90; N, 7.56. Found: C, 74.31; H, 5.01; N, 7.65. UV–vis (DMF): λ_{max}, nm 285, 312. FT-IR: υ, cm^{-1} 3399, 3311 (N − H), 3055 (=C − H), 1670 (C = O), 1283 (C = Se). ^{1}H NMR (500 MHz, $CDCl_3$): δ, ppm 11.89 (s, 1H, NH), 9.04 (s, 1H, NH), 7.77–7.72 (m, 4 H), 7.61 - 7.58 (m, 2 H), 7.52 - 7.38 (m, 8 H), 7.28 (d, J = 13.1Hz, 1H), 6.88 (s, 1H). ^{13}C NMR (125 MHz, $CDCl_3$): δ, ppm 178.3 (C = Se), 166.4 (C = O), 136.5, 133.8, 133.4, 131.8, 131.0, 129.7, 129.0, 128.8, 127.8, 127.3. LC-MS = 419.3 $[M - H]^-$.

4.1.2. N-((5H-dibenzo[a,d][7]annulen-5-yl)carbamoselenoyl)thiophene-2-carboxamide (2)

Yield: 1.20 g, 79%. Yellow solid. m.p.: 170 °C. Anal. Calc. for $C_{21}H_{16}N_2OSeS$ (%): C, 59.57; H, 3.81; N, 6.62; O, 3.78; S, 7.57. Found: C, 59.39; H, 3.29; N, 6.42; O, 3.78; S, 7.44. UV–vis (DMF): λ_{max}, nm 274, 321. FT-IR: υ, cm^{-1} 3377, 3298 (N − H), 3058 (=C − H), 1665 (C = O), 1273 (C = Se). ^{1}H NMR (500 MHz, $CDCl_3$): δ, ppm 11.28 (s, 1H, NH), 8.77 (s, 1H, NH), 7.65 (d, J = 7.2 Hz, 2H), 7.60 (d, J = 4.7 Hz, 1H), 7.56 (d, J = 2.9 Hz, 2H), 7.44 (d, J = 7.6 Hz, 3H), 7.40 (td, J = 7.5, 1.0 Hz, 3H), 7.34 (t, J = 7.1Hz, 1H), 6.79 (s, 1H), 6.37 (d, J = 2.0 Hz, 1H). ^{13}C NMR (125 MHz, $CDCl_3$): δ, ppm 177.9 (C = Se), 160.5 (C = O), 136.4, 136.1, 133.7, 131.0, 130.4, 129.7, 128.8, 128.3, 127.8. LC-MS = 407.8 $[M–H]^-$.

4.1.3. N-((5H-dibenzo[a,d][7]annulen-5-yl)carbamoselenoyl)furan-2-carboxamide (3)

Yield: 1.06 g, 76%. Pale yellow solid. m.p.: 140 °C. Anal. Calc. for $C_{21}H_{16}N_2O_2Se$ (%): C, 69.98; H, 4.47; N, 7.77; S, 8.90. Found: C, 69.82; H, 4.73; N, 7.59; S, 8.98. UV–vis (DMF): λ_{max}, nm 287, 309. FT-IR: υ, cm^{-1} 3402, 3294 (N − H), 3058 (=C − H), 1657 (C = O), 1265 (C = Se). ^{1}H NMR (500 MHz, $CDCl_3$): δ, ppm 11.64 (s, 1H, NH), 9.15 (s, 1H, NH), 7.64 (d, J = 7.3 Hz, 2H), 7.46 (s, 1H), 7.43 (d, J = 7.6 Hz, 2H), 7.41– 7.37 (m, 3 H), 7.33 (t, J = 7.5 Hz, 3 H), 7.23 (d, J = 3.0 Hz, 1H), 6.80 (s, 1H), 6.49 (d, J = 1.9 Hz, 1H). ^{13}C NMR (125 MHz, $CDCl_3$): δ, ppm 178.5 (C = Se), 156.9 (C = O), 146.1, 145.0, 136.5, 133.7, 131.0, 129.7, 128.8, 127.8, 118.3, 114.3, 113.1, 112.0. LC-MS = 425.5 $[M - H]^-$.

5. Conclusion

Spectroscopic techniques including FTIR, UV–visible, ^{1}H and ^{13}C NMR spectra were used to characterize and confirm the structure of dibenzosuberene substituted aroyl selenourea derivatives. The molecular structures were evaluated using single-crystal X-ray diffraction. Compounds **1** and **2** belong to monoclinic **(1)** and triclinic **(2)** crystal systems, with space groups P121/n1 and P-1, containing four and two molecules per unit cell, respectively. *In vitro* antimicrobial activity results revealed that compound **3** exhibited good antibacterial and antifungal activity against tested microorganisms compared to standards like Streptomycin and Nystatin. Docking results revealed that compound **3** had the least binding energy against receptor MurB with a binding energy value of –5.63 kcal/mol. The results indicate that *in silico* molecular docking studies correlated well with the experimental antibacterial activity results.

Acknowledgements

The authors Moideen Musthafa and Ramaiah Konakanchi are grateful to MHRD, Government of India, for giving a Senior Research Fellowship.

References

[1] Rayman, M. P. Selenium and Human Health. *Lancet* **2012**, *379*, 1256–1268. DOI: 10.1016/S0140-6736(11)61452-9.

[2] Ip, C. Lessons from Basic Research in Selenium and Cancer Prevention. *J. Nutr.* **1998**, *128*, 1845–1854. DOI: 10.1093/jn/128.11.1845.

[3] de Miranda, J. X.; Andrade, F. d O.; Conti, A. d.; Dagli, M. L. Z.; Moreno, F. S.; Ong, T. P. Effects of Selenium Compounds on Proliferation and Epigenetic Marks of Breast Cancer Cells. *J. Trace Elem. Med. Biol.* **2014**, *28*, 486–491. DOI: 10.1016/j.jtemb.2014.06.017.

[4] Jung, H. J.; Seo, Y. R. Current Issues of Selenium in Cancer Chemoprevention. *BioFactors* **2010**, *36*, 153–158. DOI: 10.1002/biof.81.

[5] Hughes, D. J.; Fedirko, V.; Jenab, M.; Schomburg, L.; Méplan, C.; Freisling, H.; Bueno-De-Mesquita, H. B.; Hybsier, S.; Becker, N. P.; Czuban, M.; et al. Selenium Status is Associated with Colorectal Cancer Risk in the European Prospective Investigation of Cancer and Nutrition Cohort. *Int. J. Cancer* **2015**, *136*, 1149–1161. DOI: 10.1002/ijc.29071.

[6] Dennert, G.; Zwahlen, M.; Brinkman, M.; Vinceti, M.; Zeegers, M. P. A.; Horneber, M. Selenium for Preventing Cancer. *Sao Paulo Med. J.* **2012**, *130*, 67. DOI: 10.1590/S1516-31802012000100013.

[7] Li, T.; Yi, Y.; Xu, H. Selenium-Containing Coordinating Assemblies with Selective anti-Cancer Activity: The Control of Reactive Oxygen Species. *Acta Chim. Sin.* **2014**, *72*, 1079–1084. DOI: 10.6023/A14080618.

[8] Soriano-Garcia, M. Organoselenium Compounds as Potential Therapeutic and Chemopreventive Agents: A Review. *Curr. Med. Chem.* **2004**, *11*, 1657–1669. DOI: 10.2174/0929867043365053.

[9] Frieben, E. E.; Amin, S.; Sharma, A. K. Development of Isoselenocyanate Compounds' Syntheses and Biological Applications. *J. Med. Chem.* **2019**, *62*, 5261–5275. DOI: 10.1021/acs.jmedchem.8b01698.

[10] Heimgartner, H.; Zhou, Y.; Atanassov, P. K.; Sommen, G. L. Isoselenocyanates as Building Blocks for Selenium-Containing Heterocycles. *Phosphorus Sulfur Silicon Relat. Elem.* **2008**, *183*, 840–855. DOI: 10.1080/10426500801898135.

[11] Gobouri, A. A.; Alshanbari, N. A.; Mohamed, M. A. M.; Abdel-Hafez, S. H. One Pot Synthesis of Ethyl Carboxylate and Acetyl Selenolo[2,3- b] Quinoline Derivatives and Their Tetra/Pentacyclic Systems. *Phosphorus Sulfur Silicon Relat. Elem.* **2019**, *0*, 1–7. DOI: 10.1080/10426507.2019.1662015.

[12] Ha, S. K.; Koketsu, M.; Lee, K.; Choi, S. Y.; Park, J. H.; Ishihara, H.; Kim, S. Y. Inhibition of Tyrosinase Activity by *N,N*-Unsubstituted Selenourea Derivatives. *Biol. Pharm. Bull.* **2005**, *28*, 838–840. DOI: 10.1248/bpb.28.838.

[13] Koketsu, M.; Yamamura, Y.; Aoki, H.; Ishihara, H. The Preparation of Acylselenourea and Selenocarbamate Using Isoselenocyanate. *Phosphorus Sulfur Silicon Relat. Elem.* **2006**, *181*, 2699–2708. DOI: 10.1080/10426500600862894.

[14] Alcolea, V.; Plano, D.; Karelia, D. N.; Palop, J. A.; Amin, S.; Sanmartín, C.; Sharma, A. K. Novel Seleno- and Thio-Urea Derivatives with Potent in Vitro Activities against Several Cancer Cell Lines. *Eur. J. Med. Chem.* **2016**, *113*, 134–144. DOI: 10.1016/j.ejmech.2016.02.042.

[15] Olsen, J. I.; Plata, G. B.; Padrón, J. M.; López, Ó.; Bols, M.; Fernández-Bolaños, J. G. Selenoureido-Iminosugars: A New Family of Multitarget Drugs. *Eur. J. Med. Chem.* **2016**, *123*, 155–160. DOI: 10.1016/j.ejmech.2016.07.021.

[16] Bhabak, K. P.; Satheeshkumar, K.; Jayavelu, S.; Mugesh, G. Inhibition of Peroxynitrite- and Peroxidase-Mediated Protein Tyrosine Nitration by Imidazole-Based Thiourea and Selenourea Derivatives. *Org. Biomol. Chem.* **2011**, *9*, 7343–7350. DOI: 10.1039/c1ob05773a.

[17] Hussain, R. A.; Badshah, A.; Sohail, M.; Lal, B.; Akbar, K. Synthesis, Chemical Characterization, DNA Binding and Antioxidant Studies of Ferrocene Incorporated Selenoure. *J. Mol. Struct.* **2013**, *1048*, 367–374. DOI: 10.1016/j.molstruc.2013.06.004.

[18] Merino-Montiel, P.; Maza, S.; Martos, S.; López, Ó.; Maya, I.; Fernández-Bolaños, J. G. Synthesis and Antioxidant Activity of O-Alkyl Selenocarbamates, Selenoureas and Selenohydantoins. *Eur. J. Pharm. Sci.* **2013**, *48*, 582–592. DOI: 10.1016/j.ejps.2012.12.016.

[19] Aller, A. J.; Robles, L. C. Speciation of Selenomethionine and Selenourea Using Living Bacterial Cells. *Analyst* **1998**, *123*, 919–927. DOI: 10.1039/a707696g.

[20] Díaz, M.; H. De, L.; Moreno, E.; Espuelas, S.; Aydillo, C.; Jiménez-Ruiz, A. Crossm Synthesis and Leishmanicidal Activity of Novel Urea, Thiourea,. *Antimicrob. Agents Chemother* **2019**, *63*, 1–16.

[21] Tuchila, C.; Baconi, D.; Pirvu, C.; Balalau, D.; Vlasceanu, A.; Stan, M.; Balalau, C. Therapeutic Drug Monitoring and Methods of Quantitation for Carbamazepine. *J. Mind Med. Sci.* **2017**, *4*, 100–114. DOI: 10.22543/7674.42.P100114.

[22] Burbiel, J. C. On the Syntheses of Dibenzosuberenone and 2,8-Dimethyl-Dibenzosuberenone. *Arkivoc* **2006**, *2006*, 16–21. DOI: 10.3998/ark.5550190.0007.d03.

[23] Merkaš, S.; Litvić, M.; Cepanec, I.; Vinković, V. Synthesis of Novel, Potentially Biologically Active Dibenzosuberone Derivatives. *Molecules* **2005**, *10*, 1429–1437. DOI: 10.3390/10121429.

[24] Koeberle, S. C.; Fischer, S.; Schollmeyer, D.; Schattel, V.; Grütter, C.; Rauh, D.; Laufer, S. A. Design, Synthesis, and Biological Evaluation of Novel Disubstituted Dibenzosuberones as Highly Potent and Selective Inhibitors of P38 Mitogen Activated Protein Kinase. *J. Med. Chem.* **2012**, *55*, 5868–5877. DOI: 10.1021/jm300327h.

[25] Rohini, G.; Haribabu, J.; Sheeba, M. M.; Aneesrahman, K. N.; Bhuvanesh, N. S. P.; Balachandran, C.; Karvembu, R.; Sreekanth, A. Ru(II)-Η6-Benzene Complexes of Dibenzosuberenyl Appended Aroyl/Acylthiourea Ligands: In Vitro Biomolecular Interaction Studies and Catalytic Transfer Hydrogenation. *ChemistrySelect* **2018**, *3*, 18–28. DOI: 10.1002/slct.201702538.

[26] Musthafa, M.; Aneesrahman, K. N.; Perumalsamy, B.; Ramasamy, T.; Ganguly, R.; Sreekanth, A. Synthesis, Crystal Structure, DFT Study, in Vitro and in Silico Molecular Docking of Novel Bis (Aroyl Selenourea) Derivatives. *J. Mol. Struct.* **2019**, *1180*, 585–594. DOI: 10.1016/j.molstruc.2018.12.019.

[27] Hussain, R. A.; Badshah, A.; Shah, A. Synthesis and Biological Applications of Selenoureas. *Appl. Organometal. Chem.* **2014**, *28*, 61–73. DOI: 10.1002/aoc.3093.

[28] Molter, A.; Rust, J.; Lehmann, C. W.; Mohr, F. Synthesis and Structural Studies of Some Selenoureas and Their Metal Complexes. *Arkivoc* **2011**, *vi*, 10–17.

[29] Lone, S. H.; Jameel, S.; Bhat, M. A.; Lone, R. A.; Butcher, R. J.; Bhat, K. A. Synthesis of an Unusual Quinazoline Alkaloid: Theoretical and Experimental Investigations of Its Structural, Electronic, Molecular and Biological Properties. *RSC Adv.* **2018**, *8*, 8259–8268. DOI: 10.1039/C8RA00138C.

[30] Li, Y.; Liu, Y.; Wang, H.; Xiong, X.; Wei, P.; Li, F. Synthesis, Crystal Structure, Vibration Spectral, and DFT Studies of 4-Aminoantipyrine and Its Derivatives. *Molecules* **2013**, *18*, 877–893. DOI: 10.3390/molecules18010877.

[31] Costa, R. A.; Oliveira, K. M. T.; Costa, E. V.; Pinheiro, M. L. B. Vibrational, Structural and Electronic Properties Investigation by DFT Calculations and Molecular Docking Studies with DNA Topoisomerase II of Strychnobrasiline Type Alkaloids: A Theoretical Approach for Potentially Bioactive Molecules. *J. Mol. Struct.* **2017**, *1145*, 254–267. DOI: 10.1016/j.molstruc.2017.05.087.

[32] Ramaiah, K.; Prashanth, J.; Haribabu, J.; Srikanth, K. E.; Venkatram Reddy, B.; Karvembu, R.; Laxma Reddy, K. Vibrational Spectroscopic (FT-IR, FT-Raman), anti-Inflammatory, Docking and Molecular Characteristic Studies of Ni(II) Complex of 2-Aminonicotinaldehyde Using Theoretical and Experimental Methods. *J. Mol. Struct.* **2019**, *1175*, 769–781. DOI: 10.1016/j.molstruc.2018.08.044.

[33] Eswar Srikanth, K.; Ramaiah, K.; Jagadeeswara Rao, D.; Prabhakara Rao, K.; Laxman Naik, J.; Veeraiah, A.; Prashanth, J. Experimental and Theoretical Analyses on Structural (Monomer and Dimeric Form), Spectroscopic and Electronic Properties of an Organic Semiconductor 2,6-Dimethoxyanthracene. *Indian J. Phys.* **2019**, DOI: 10.1007/s12648-019-01562-z.

[34] Gece, G. The Use of Quantum Chemical Methods in Corrosion Inhibitor Studies. *Corros. Sci.* **2008**, *50*, 2981–2992. DOI: 10.1016/j.corsci.2008.08.043.

[35] Fukui, K. Role of Frontier Orbitals in Chemical Reactions. *Science* **1982**, *218*, 747–754. DOI: 10.1126/science.218.4574.747.

[36] Choi, C. H.; Kertesz, M. Conformational Information from Vibrational Spectra of Styrene, Trans-Stilbene, and Cis-Stilbene. *J. Phys. Chem. A* **1997**, *101*, 3823–3831. DOI: 10.1021/jp970620v.

[37] Sivagami, G.; Vinothkumar, R.; Preethy, C. P.; Riyasdeen, A.; Akbarsha, M. A.; Menon, V. P.; Nalini, N. Role of Hesperetin (a Natural Flavonoid) and Its Analogue on Apoptosis in HT-29 Human Colon Adenocarcinoma Cell Line - A Comparative Study. *Food Chem. Toxicol.* **2012**, *50*, 660–671. DOI: 10.1016/j.fct.2011.11.038.

[38] Koopmans, T. Über Die Zuordnung Von Wellenfunktionen Und Eigenwerten Zu Den Einzelnen Elektronen Eines Atoms. *Physica* **1934**, *1*, 104–113. DOI: 10.1016/S0031-8914(34)90011-2.

[39] Parr, R. G.; Szentpály, L. V.; Liu, S. Electrophilicity Index. *J. Am. Chem. Soc.* **1999**, *121*, 1922–1924. DOI: 10.1021/ja983494x.

[40] Suganthi, S.; Balu, P.; Sathyanarayanamoorthi, V.; Kannappan, V.; Kamil, M. G. M.; Kumar, R. Structural Analysis and Investigation of Molecular Properties of Cefpodoxime Acid, a Third Generation Antibiotic. *J. Mol. Struct.* **2016**, *1108*, 1–15. DOI: 10.1016/j.molstruc.2015.11.069.

[41] Kumar, V.; Saravanan, P.; Arvind, A.; Mohan, C. G. Identification of Hotspot Regions of MurB Oxidoreductase Enzyme Using Homology Modeling, Molecular Dynamics and Molecular Docking Techniques. *J. Mol. Model.* **2011**, *17*, 939–953. DOI: 10.1007/s00894-010-0788-3.

[42] Ragunathan, A.; Malathi, K.; Anbarasu, A. MurB as a Target in an Alternative Approach to Tackle the Vibrio Cholerae Resistance Using Molecular Docking and Simulation Study. *J. Cell. Biochem.* **2018**, *119*, 1726–1732. DOI: 10.1002/jcb.26333.

[43] Settypalli, T.; Chunduri, V. R.; Kerru, N.; Nallapaneni, H. K.; Chintha, V. R.; Daggupati, T.; Yeguvapalli, S.; Wudayagiri, R. Design, Synthesis, Neuroprotective and Antibacterial Activities of 1,2,4-Triazolo[3,4-b]1,3,4-Thiadiazole Linked Thieno[2,3-d]Pyrimidine Derivatives and in Silico Docking Studies. *ChemistrySelect* **2019**, *4*, 1627–1634. DOI: 10.1002/slct.201803917.

[44] Konakanchi, R.; Haribabu, J.; Prashanth, J.; Nishtala, V. B.; Mallela, R.; Manchala, S.; Gandamalla, D.; Karvembu, R.; Reddy, B. V.; Yellu, N. R.; et al. Synthesis, Structural, Biological Evaluation, Molecular Docking and DFT Studies of Co(II), Ni(II), Cu(II), Zn(II), Cd(II) and Hg(II) Complexes Bearing Heterocyclic Thiosemicarbazone Ligand. *Appl. Organomet. Chem.* **2018**, *32*, 1–18. DOI: 10.1002/aoc.4415.

[45] Munikumari, G.; Konakanchi, R.; Nishtala, V. B.; Ramesh, G.; Kotha, L. R.; Chandrasekhar, K. B.; Ramachandraiah, C. Palladium(II) Complexes of 5-Substituted Isatin Thiosemicarbazones: Synthesis, Spectroscopic Characterization, Biological Evaluation and in Silico Docking Studies. *Synth. Commun.* **2019**, *49*, 146–158. DOI: 10.1080/00397911.2018.1546400.

[46] Konakanchi, R.; Mallela, R.; Guda, R.; Kotha, L. R. Synthesis, Characterization, Biological Screening and Molecular Docking Studies of 2-Aminonicotinaldehyde (ANA) and Its Metal Complexes. *Res. Chem. Intermed.* **2018**, *44*, 27–53. DOI: 10.1007/s11164-017-3089-y.

[47] Rohini, G.; Ramaiah, K.; Aneesrahman, K. N.; Aryasenan, M. C.; Bhuvanesh, N. S. P.; Reddy, K. L.; Sreekanth, A. Biological Evaluation, DNA/Protein-Binding Aptitude of Novel Dibenzosuberene Appended Palladium (II)-Thiourea Complexes. *Appl. Organomet. Chem.* **2018**, *32*, 1–12. DOI: 10.1002/aoc.4567.